Observations of the 26 August 2018 Geomagnetic Storm

Whitham D. Reeve

1. Introduction

The current sunspot cycle continues to wind down but it still produces significant events. This happened on 26 August 2018 when parts of a coronal mass ejection (CME) collided with Earth's magnetosphere causing a major geomagnetic storm. CMEs are comparatively rare during the Sun's downward cycle because they most often are associated with flares or filament eruptions, both of which are relatively rare in the low part of the cycle. In this case, the CME was thought to be associated with a filament eruption on 20 August (figure 1). The CME itself was too weak to be automatically detected by satellites designed for that purpose. After additional manual analysis the CME was estimated to have only minor Earth-directed parts. However, its effects were not minor. What actually happened is discussed in this report.

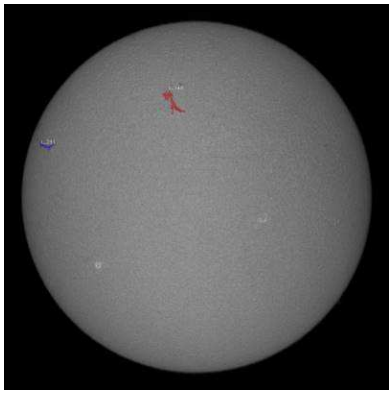

Figure 1 ~ Image of the Sun at 546 nm wavelength. The 20 August filament thought to be the origin of the CME is seen in the upper part of the image to the left of the central meridian and marked in red. There were no flares on this day. Image source: Kanzelhöhe Observatory in Austria {KSO}

2. Magnetic Field Components and Disturbances

CMEs carry with them parts of the Sun's magnetic field – the field is said to be *frozen in*. The Geocentric Solar Magnetospheric System (GSM) is a coordinate system commonly used to describe the magnetic field components in the space between Sun and Earth, called *Interplanetary Magnetic Field* or IMF. These components are labeled Bx, By and Bz (figure 2). The Bz component of the embedded magnetic field is by definition aligned with Earth's magnetic dipole field. If the CME's Bz component has opposite polarity, called southward or negative Bz, the CME's and Earth's magnetic fields can merge in a process called *magnetic reconnection*. During the 26 August event, Bz was in the range –15 to –17 nT throughout most of the day and, thus, enabled reconnection. Reconnection can release large amounts of magnetic energy and strongly disturb Earth's magnetosphere.

A CME's collision with Earth's magnetosphere often results in a *sudden impulse*, but an SI was neither reported by Space Weather Prediction Center (SWPC) nor visible in the Anchorage magnetogram for the 26 August event, possibly because the CME was a slow glancing blow. Geomagnetic storms are often enhanced by high solar wind speeds; however, on 26 August, the speed was a nominal 463 km s^{-1} at first but increased later in the day to a maximum of 566 km s^{-1} due to a coronal hole high-speed stream {SWPC}. A plot of Bz and solar wind speed from

the DSCOVR spacecraft shows the trends in IMF Bz and speed (figure 3). The speed increase apparently did not influence or prolong the storm and Earth's magnetic field was back to normal by the end of the day.

The degree of magnetic disturbance is commonly measured in 3 hour synoptic periods by the quasi-logarithmic scale called the *K-index*. The K-index ranges from K0 (very quiet) to K9 (very disturbed). The K-index in professional observatories is based on calculations of variations in the horizontal component of the magnetic field measured on Earth's surface. The horizontal component is the vector sum of terrestrial Bx (north-south) and By (east-west) components (note that these field designations are different than the IMF components defined by the GSM discussed above).

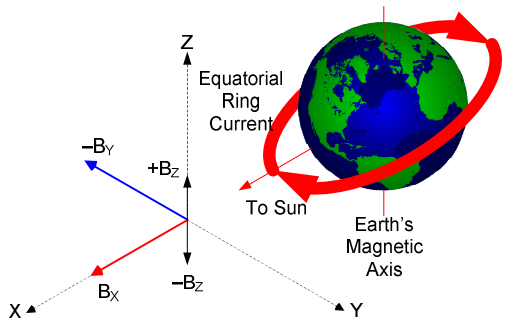

Figure 2 ~ The Geocentric Solar Magnetospheric System (GSM) shown here is one of many reference systems used to study Sun-Earth magnetic field relationships. The GSM has its X-axis pointed away from Earth to the Sun, and the Y-axis is perpendicular to Earth's magnetic dipole so that the X-Z plane contains the dipole axis. The positive Z-axis is chosen to be in the same sense as the northern magnetic pole. The corresponding components of magnetic induction are named Bx, By and Bz. Also shown is a representation of the equatorial ring current (discussed later). Image © 2018 W. Reeve

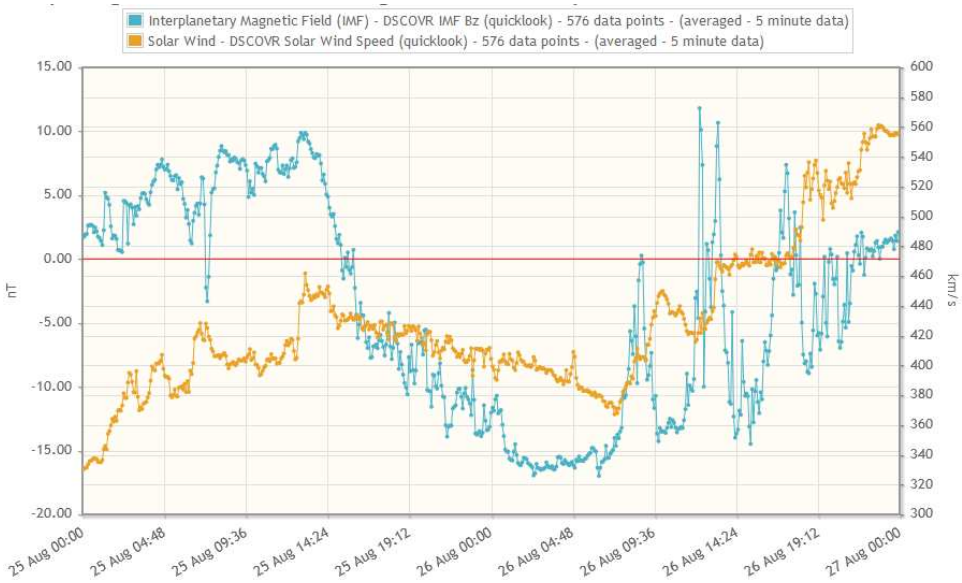

Figure 3 ~ 48 h plot of solar wind speed (gold trace, right scale) and IMF Bz component (blue trace, left scale) from DSCOVR spacecraft for 25-26 August. DSCOVR is located 1.5 million km from Earth on the Earth-Sun line. Note the decrease in Bz to negative values starting about 1500 UTC on 25 August. The disturbance on Earth sharply escalated about 10 h later. Image source: Solar Timelines viewer for AFFects {STAFF}

Another useful index that indicates the severity of a geomagnetic storm is the *Dst* or *Disturbance storm-time index*. The Dst index is based on hourly magnetic measurements at low-latitude observatories. It shows the effect of the westward flowing equatorial ring current on the surface magnetic field. The ring current consists of a toroidal band of ions (mostly protons, which have a positive charge) in the equatorial plane at a distance ranging from about 3 to 8 Earth radii ($R_E \approx 6370$ km). The charged particles are trapped on Earth's magnetic field lines and drift as Earth rotates. The moving charges produce a magnetic field that opposes Earth's magnetic field. Therefore, an increase in the ring current caused by a magnetic disturbance is observed as a decrease in

Earth's magnetic field, particularly the horizontal component measured on Earth's surface. During magnetically quiet times the Dst is near zero and then becomes negative with the storm.

3. Observations

The SAM-III magnetometer at Anchorage runs continuously and is described in {ReeveSI}. It recorded a comparatively quiet day on 25 August (figure 4) for comparison with the major storm that followed the next day 26 August (figure 5). These magnetograms show magnetic induction values that have been normalized at the beginning of the UTC day. Thus, a positive value on the magnetogram represents an increase in magnetic induction with respect to the value measured at the previous midnight. The polar plots shown with the magnetograms are another way of displaying how the magnetic field has changed during the day but they have no time scale.

The magnetograms also display the K-index for each 3 h period. The K-index calculations in the SAM-III differ from professional observatories discussed in section 2. The SAM-III calculates a K-index for each component (terrestrial values of Bx, By and Bz) and not the horizontal component. On 26 August the Anchorage K-index reached its highest possible value (K9) during the 0600 to 0900 UTC synoptic interval with K6, K7 and K8 at other times throughout the day. Although the SAM-III K-index calculations are slightly different than professional observatories, the values still are comparable. For example, the high-latitude observatory at College, Alaska (station CMO) about 400 km north of Anchorage published K8 for the 0600 to 0900 UTC period and K5, K6 and K7 for the other times {DGD}. The mid-latitude station at the Fredericksburg Geomagnetic Observatory in Virginia (station FRD) published K6 and K4 and K5 for the same periods. These types of differences often occur between lower and higher latitude observatories.

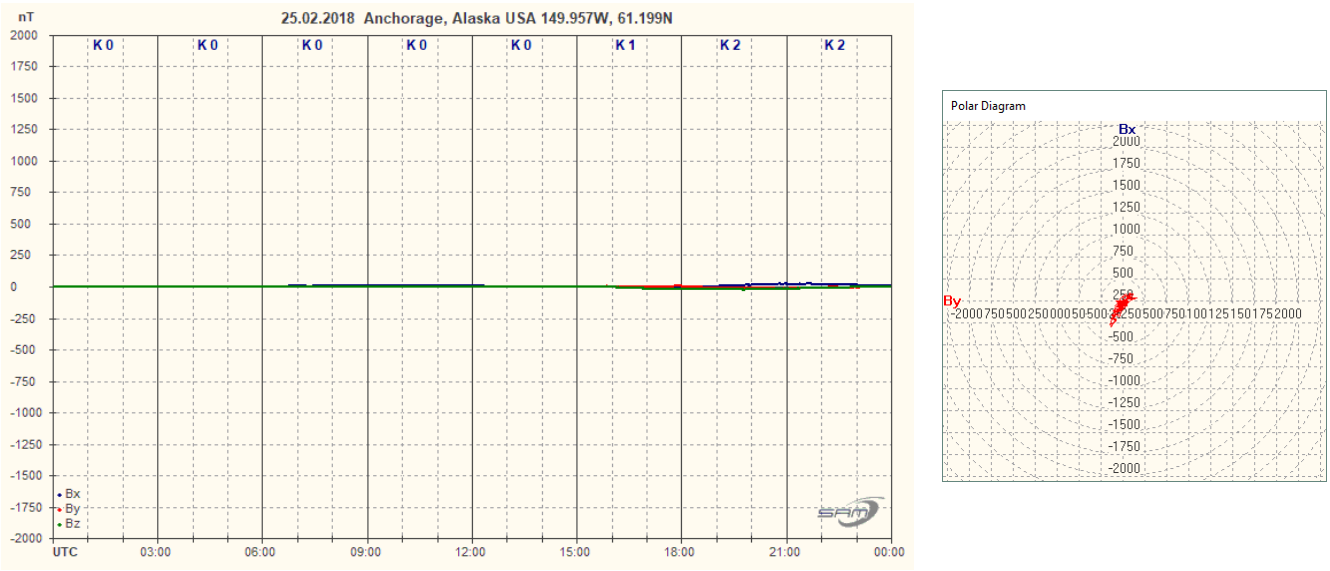

Figure 4 ~ Left: Anchorage magnetogram for 25 August indicating a quiet day with only a very minor disturbance during the last 6 h of the day as the CME started to influence the magnetosphere. The vertical scale shows magnetic induction in nT and the horizontal scale shows time in UTC. The K-index for each 3 h synoptic period is shown along the top of the plot. The values shown here are the highest of the computed K-index for Bx, By and Bz. Right: Polar diagram showing Bx and By for 25

August. Although the polar plot does not have a time scale, the individual Bx and By values and corresponding times can be read at any time by hovering the mouse over the trace when running the SAM_VIEW software. Images © 2018 W. Reeve

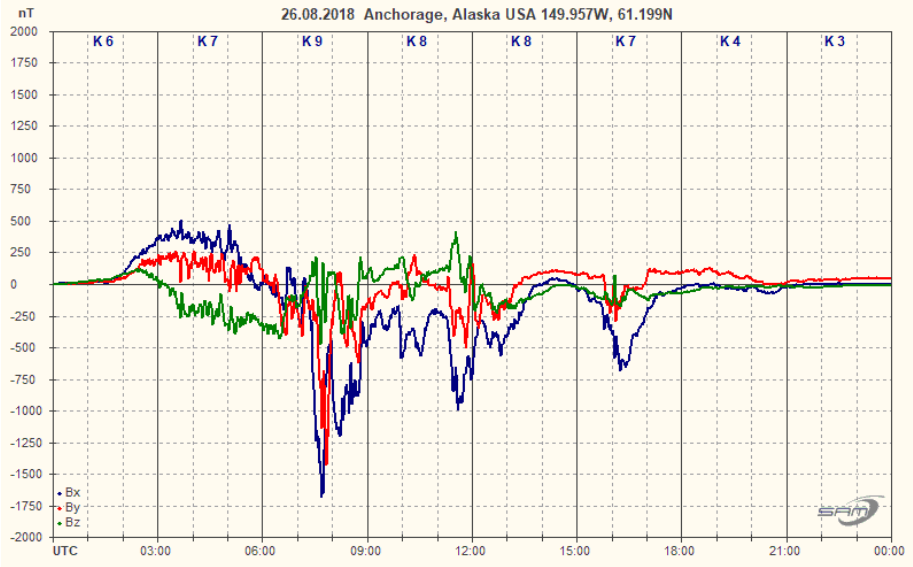

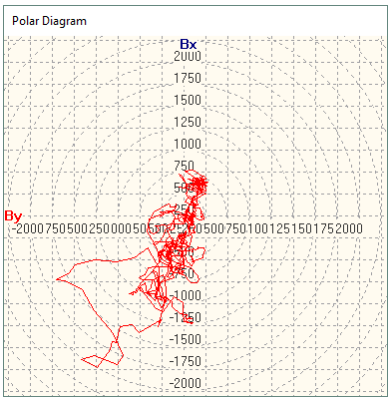

Figure 5 ~ Left: Anchorage magnetogram for 26 August indicating the onset of the geomagnetic storm at about 0100 UTC. This plot uses the same vertical scale as the previous figure. The storm intensity peaked about 0730 and started to quiet down about 1700, returning to an almost fully quiet level by the end of day. Right: Polar diagram for 26 August showing the wide negative excursions in both Bx (north-south) and By (east-west). Images © 2018 W. Reeve

For comparison I have included magnetograms for two other locations in Alaska, Trapper Creek and Gakona (figure 6). These magnetometers are operated by the University of Alaska Geophysical Institute. The UAF-GI magnetometers use a different reference system (H, D and Z) than the SAM-III (X, Y and Z). However, the overall activity is very similar except that individual features such as peaks may be plotted at different times. For more information on reference systems, see {Reeve15}.

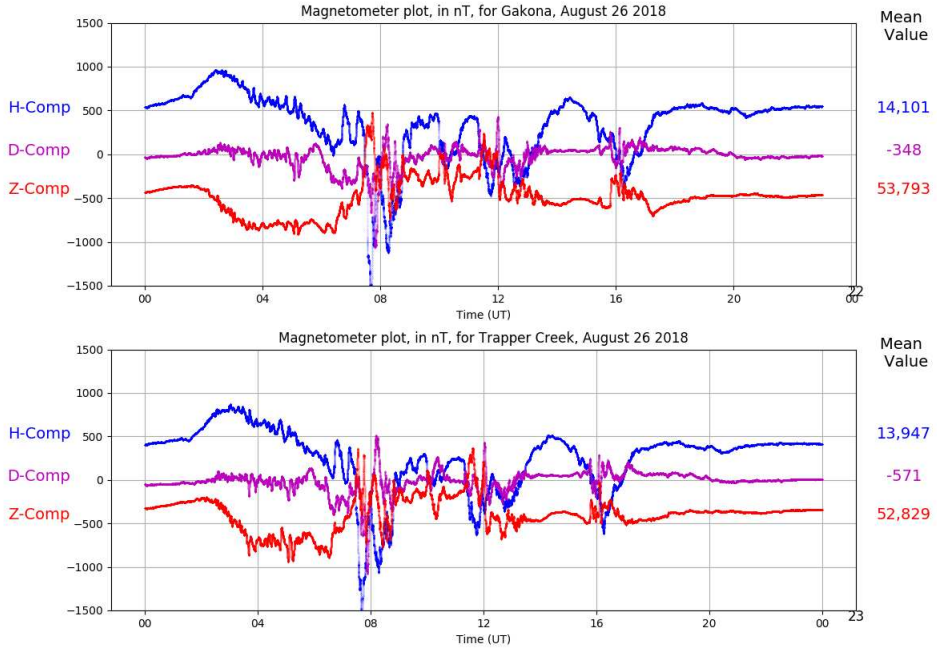

Figure 6 ~ Magnetograms for 26 August from magnetometers operated by University of Alaska Geophysical Institute. These magnetograms show horizontal (H, vector sum of Bx and By), variation in the declination displayed in nT (D) and vertical (Z) magnetic components.

Upper: Gakona, Alaska at latitude 62°N about 285 km east-northeast of Anchorage. Lower: Trapper Creek, Alaska at latitude 62°N, about 130 km north of Anchorage.

Images source: {UAFGI-Mag}

The Dst-index data from the *World Data Center for Geomagnetism* at Kyoto University indicates a sharp drop on 26 August and a slow recovery afterwards (figure 7). The Dst-index reached a minimum of –171 nT during the 0700 UTC hour on 26 August {WDC-Kytoto}. These data are from equatorial observatories; my observatory in Anchorage is too far north to reliably measure the Dst-index.

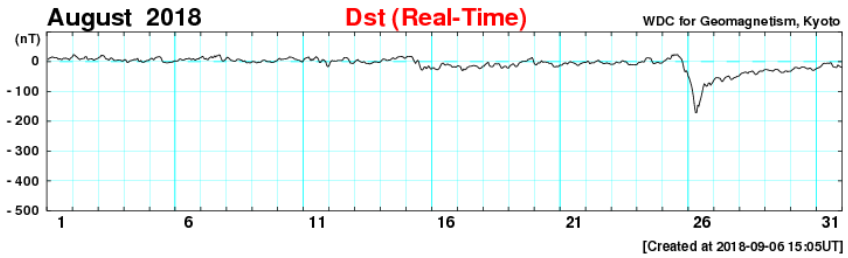

Figure 7 ~ Dst-index plot for the entire month of August 2018. Note the values are near zero for the whole month until the sharp dip on 26 August. The magnetic field had not yet fully returned to normal by end of month. Image source: {WDC-Kytoto}

The *Solar-Terrestrial Centre of Excellence* (STCE) recently published a table of all magnetic storm events with Dst values of –100 nT or lower in the current solar cycle (table 1). The table includes the planetary Kp-index, the local K-index recorded at Dourbes Belgium {Dourbes, latitude 50° north} and the source of the geomagnetic storm. The Kp-index is the average of eight observatories throughout the world at various latitudes. The vast majority of storms are due to CMEs (indicated as *interplanetary* CMEs in the table) but a few were due to coronal hole high-speed streams in conjunction with a corotating interaction region (indicated as CH CIR). Corotating interaction regions are locations in the solar wind where particles and the IMF pile-up as lower speed streams are overtaken by higher-speed streams from coronal holes.

Event date	Dst min	Kp final	K Dourbes	Source
17-18 March 2015	-223	8-	7	ICME
22-23 June 2015	-204	8+	8	ICME
26 August 2018	-169	7	6	ICME
20-21 December 2015	-155	7-	6	ICME
25 October 2011	-147	7+	7	ICME
9 March 2012	-145	8	6	ICME
15-16 July 2012	-139	7	6	ICME
17 March 2013	-132	7-	6	ICME
28 May 2017	-125	7	6	ICME
1 June 2013	-124	7	6	CH CIR
7 October 2015	-124	7+	6	CH CIR
8 September 2017	-124	8+	6	ICME
1 October 2012	-122	7-	5	ICME
23-24 April 2012	-120	7-	5	ICME
19 February 2014	-119	6+	5	ICME
26-27 September 2011	-118	6+	6	ICME
5-6 August 2011	-115	8-	6	ICME
1 January 2016	-110	6	5	ICME
8-9 October 2012	-109	7-	5	ICME
14 November 2012	-108	6+	5	ICME
13 October 2016	-104	6+	5	ICME
29 June 2013	-102	6+	5	CH CIR

Table 1 ~ Geomagnetic storms during solar cycle 24 in which the decrease in the horizontal component of Earth's magnetic field, as measured by the Dst-index, exceeded –100 nT. Other data is shown for comparison: Kp is the planetary K-index and K Dourbes is a local K-index in Belgium. The disturbances are caused by ICME, interplanetary coronal mass ejection, and CH CIR, coronal hole high-speed stream following a corotating interaction region. Table source: {SCTE}

The table indicates that the geomagnetic storm on 26 August is, in terms of the Dst-index, the third strongest of the current solar cycle. The Dst-index for 26 August was lower only for the geomagnetic storms on 17-18 March 2015 and 22-23 June 2015. The small difference between the Dst-index shown in the table (–169) and the value

indicated at WDC-Kyoto (–171), noted above, is probably due to updates made to the latter after the SCTE table was prepared.

4. Space Weather

Bad space weather such as an Earth-directed coronal mass ejection can negatively affect spacecraft, radio propagation and electric and telecommunications infrastructure. These effects are well documented; for example, see [Kippler].Probably the only positive effect of space weather disturbances is the increased chance of aurora viewing at latitudes lower than normal. Although the terrestrial cloud cover was very low in Anchorage in late August, I did not stay up late enough to view the aurora from the 26 August storm.

University of Alaska Geophysical Institute provides worldwide daily forecasts for aurora viewing based on the expansion of the auroral oval during a geomagnetic storm {AuroraFcst}. Archived data for 26 and 27 August shows that the viewing forecast for the day of the geomagnetic storm was low for areas outside the *normal* auroral oval but increased significantly the next day (figure 8). Incidentally, the SAM magnetometer was originally designed for detection of conditions conducive to auroral viewing and enhanced radio propagation that might be associated with a geomagnetic storm.

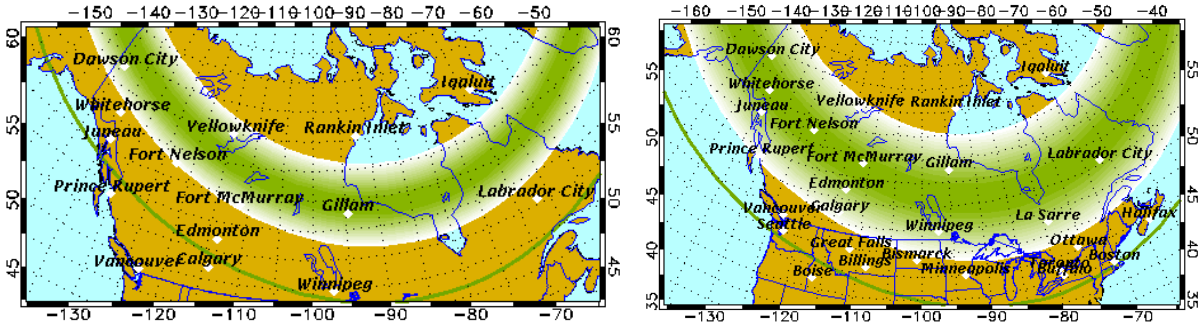

Figure 8 ~ Auroral oval forecasts for North America (maps for other areas of the world are available). Left: 26 August, day of the geomagnetic storm, the forecast was for low activity; Right: 27 August, day after the geomagnetic storm, the forecast was for high activity with viewing in some of the northern lower-48 states. Images source: {AuroraFcst}

5. Conclusions

Solar cycle 24 continues to produce surprises, in this case a strong geomagnetic storm on 26 August 2018. The cycle has not yet reached a minimum and overall solar activity will continue to drop until the minimum is reached. However, additional outbursts may take place. Having the instrumentation to record and analyze geomagnetic activity and having easy access to worldwide data associated with geomagnetic conditions for comparison is more fun than a dancehall riot.

6. References & Weblinks

{AuroraFcst} http://auroraforecast.gi.alaska.edu/?area=NorthAmerica

{DGD} ftp://ftp.swpc.noaa.gov/pub/indices/old_indices/2018Q3_DGD.txt

{Dourbes} http://ionosphere.meteo.be/geomagnetism/ground_K_dourbes/

[Knipp] Knipp, D., Understanding Space Weather and the Physics Behind It, McGraw-Hill, 2011, ISBN 978-0-07-340890-3

{KSO} http://cesar.kso.ac.at/sn_iv/filament_data.php?date=20180820

{Reeve15} Reeve, W., Geomagnetism Tutorial, 2015, available at: http://www.reeve.com/Documents/SAM/GeomagnetismTutorial.pdf

{ReeveSI} Reeve, W., Geomagnetic Sudden Impulses, available at: http://www.reeve.com/Documents/Articles%20Papers/Observations/Reeve_GeomagSuddenImpulses.pdf

{SCTE} STCE newsletter, 31 Aug 2018. The Solar-Terrestrial Centre of Excellence is a collaborative network of the Belgian Institute for Space Aeronomy, the Royal Observatory of Belgium and the Royal Meteorological Institute of Belgium. Available at: http://www.stce.be/newsletter/pdf/2018/STCEnews20180831.pdf

{STAFF} http://www.staff.oma.be

{SWPC} ftp://ftp.swpc.noaa.gov/pub/forecasts/discussion/08270030forecast_discussion.txt

{UAFGI-Mag} http://www.gi.alaska.edu/magnetometer/archive

{WDC-Kyoto} http://wdc.kugi.kyoto-u.ac.jp/dst_realtime/201808/index.html

Author - Whitham Reeve is a contributing editor for the SARA journal, Radio Astronomy. He obtained B.S. and M.S. degrees in Electrical Engineering at University of Alaska Fairbanks, USA. He worked as a professional engineer and engineering firm owner/operator in the airline and telecommunications industries for more than 40 years and now manufactures electronic equipment used in radio astronomy. He has lived in Anchorage, Alaska his entire life. Email contact: whitreeve@gmail.com